

Simulation of Coherent Synchrotron Radiation Emission from Rotating Relativistic Electron Layers

Bjoern S. Schmekel

*Department of Physics, Cornell University, Ithaca, New York 14853**

The electromagnetic radiation of a rotating relativistic electron layers is studied numerically using particle-in-cell simulation. The results of the simulation confirm all relevant scaling properties predicted by theoretical models. These models may turn out to be important for the understanding of the coherent synchrotron radiation (CSR) instability that may occur in systems as diverse as particle accelerators radio pulsars.

Extremely high brightness temperatures encountered for example in the radio emission of pulsars cannot be explained by an incoherent radiation mechanism for which the radiated power is proportional to the number of radiating charges. However, if all outgoing waves interfere constructively the total power scales as the square of that number. In future particle accelerators the wavelength of the emitted radiation can easily reach the length of the accelerated bunches such that bunches can modulate themselves by means of their own radiation. The possible energy loss caused by CSR would be undesirable for the operation of such accelerators.

The aim of the present work is to test the results obtained from the model developed by Schmekel, Lovelace and Wasserman [1] numerically. The model predicts growth rates and saturation amplitudes (among other quantities) for an initial perturbation of a rotating relativistic cylinder of charged particles in an external magnetic field. The linear instability is closely related to the instability found by Goldreich and Keeley [2]. The distribution function is chosen such that the azimuthal canonical angular momentum is fixed and the energy drops off exponentially. For the time being all fields and distribution functions are assumed to be uniform in the z -direction. The equilibrium can be parametrized by the radius r_0 of the cylinder, the relative energy spread v_{th}^2 of the particles, the Lorentz factor γ (with $c = 1$) and the dimensionless field reversal parameter

$$\zeta \equiv \frac{4\pi en_0 r_0 v_{th} \sqrt{\pi/2}}{B_z^{ext}}, \quad (1)$$

where n_0 is the central number density, v_ϕ the azimuthal velocity and B_z^{ext} the external magnetic field in the z -direction in cgs units. Considering all perturbed quantities to have the dependence $\exp(im\phi - i\omega t + k_r r)$ we obtained for $m^{2/3} v_{th} \ll 1$ and $k_r v_{th} r_0 \ll 1$, the growth rate

$$\Im(\omega) \simeq \frac{1.083 \zeta^{1/2} m^{2/3} \dot{\phi}}{\gamma} \sqrt{F_0}, \quad (2)$$

and

$$\Re(\omega) \simeq \frac{\zeta^{1/2} m^{1/2} \dot{\phi}}{\gamma^{1/2}} \sqrt{F_0},$$

for $m \gg 2\gamma^3 \equiv m_2$ where $\dot{\phi}$ is the angular velocity, the dot denotes the time derivative, and

$$F_0 \equiv \frac{1}{2\pi} \int_{-\pi}^{\pi} e^{-\frac{m^2 v_{th}^2}{2} (1-\sin\theta)^2} d\theta. \quad (3)$$

The saturation amplitude of the electric field $|E|$ is

$$|\delta E_{sat}|^2 = \left(\frac{m_e \gamma}{e r_0 m}\right)^2 \left(\frac{\Im(\omega)(m)}{\dot{\phi}}\right)^4, \quad (4)$$

where m_e is the mass of the electron and the radiated power is given by

$$P_m \approx 3.71 \times 10^{14} \gamma^6 m^{-3} \frac{L}{r_0} \left(\frac{\Im(\omega)}{\dot{\phi}}\right)^4 \frac{\text{erg}}{s}. \quad (5)$$

Here the length of the cylindrical layer is denoted by L . As was shown in [1] we will later have to replace L by r_0 in order to compute the growth for a thin ring. The quoted expressions were derived by approximating Bessel functions with Airy functions. It was shown that this approximation is valid under the conditions $m \gg 1$ and $m \gg \zeta^{3/2} \gamma^3 \equiv m_1$. However, evaluating the dispersion relation numerically it is found that those expressions are still good approximations if these conditions are not satisfied.

Two different software packages were considered. TraFiC⁴ 2.0 [3] is a program that was specifically designed for CSR simulations for particle accelerators. It is very memory efficient and very useful if one has a very specific set-up of dipole, quadrupole and sextupole magnets etc. However, it appeared to be problematic to make TraFiC4 deal with the model in [1]. Also, post-processing the output is far more difficult than with the general purpose code OOPIC [4] which was finally chosen. OOPIC is a relativistic two-dimensional particle-in-cell code which supports both plain (x, y) -geometries and cylindrical (r, z) -geometries. Since the interesting dynamics takes places in the azimuthal direction one would have to simulate a thin ring (instead of a cylinder) in the (x, y) -mode. Loading the initial circular particle distribution in the (x, y) -mode required modifying the source code to allow the program to handle circular particle distributions. Another consideration is the

memory requirement since a very fine mesh is needed for CSR simulations.

The simulations were performed on the author's Sun workstation. The workstation is a Sun Blade 100 with a single 500MHz UltraSPARC II CPU and 1664MB of main memory running SunOS 5.9 / Solaris 9. Some minor modifications were necessary in order to compile XOOPIC-2.5.1 with gcc 3.2.2. The built-in function parser was extended to support elliptic integrals and other useful functions and recompiled with the compiler compiler bison 1.28. Furthermore, the files load.cpp, diagn.cpp and c_utils.c had to be changed to simplify loading circular distribution functions and postprocessing of the output. Since we simulate a thin ring instead of a cylinder all fields and charges have to be divided by the length L of the cylinder whereas the electron mass needs to be divided by L^2 . $L = 10r_0$ is chosen unless noted otherwise. The electric and magnetic self-fields for a thin ring equilibrium differ from what was used in the model [1]. The fields can be found in [5]. It is ensured that OOPIC uses these self-fields before the perturbation starts to build up. As it turns out choosing the correct self-fields is not too crucial. Leaving them out the system will build them up itself. Once the self-fields are created the system shows no difference in behavior. The absence of the self-fields in the dispersion relation [1] might help to understand this feature. As in [1] a Gaussian number density profile with RMS width v_{th} was chosen for the initial distribution. 5000 macro particles were tracked on a grid with resolution 512×512 unless noted otherwise. Once an energy for a particle has been chosen it is placed at the equilibrium radius $r_0 = m\gamma c(eB)^{-1}$, i.e. neglecting betatron oscillations particles on the same orbit have the same energy. This fixes the azimuthal component of the canonical angular momentum. The system can pick up transverse motion quickly. The grid represents a rectangular region $40m \times 40m$ big. The ring with radius $r_0 = 10m$ is centered in the grid.

In Fig. 1 the initial particle distribution (gray) and the particle distribution after $23ns$ are shown. The parameters are $\zeta = 0.010$, $\gamma = 30$, and $v_{th} = 0.002$. Qualitatively, a bunching of the particle distribution can be observed. An enlargement of a small section of fig. 1 is also shown in the same figure. Also note that during the evolution of the circular charge distribution both the radius and the width of the ring increase slightly. The former is due to a.) particles losing energy and b.) the magnetic self-field changing significantly. It tends to decrease for small energy spreads and increase for larger energy spreads. Since the non-zero mesh size imposes an upper limit on the azimuthal mode number m which can become unstable, it is expected that the distance between bunches decreases as the resolution increases. This is indeed the case. The bunches are slightly tilted and may be connected by a very thin inner ring of particles for sufficiently high beam currents. For these reasons it

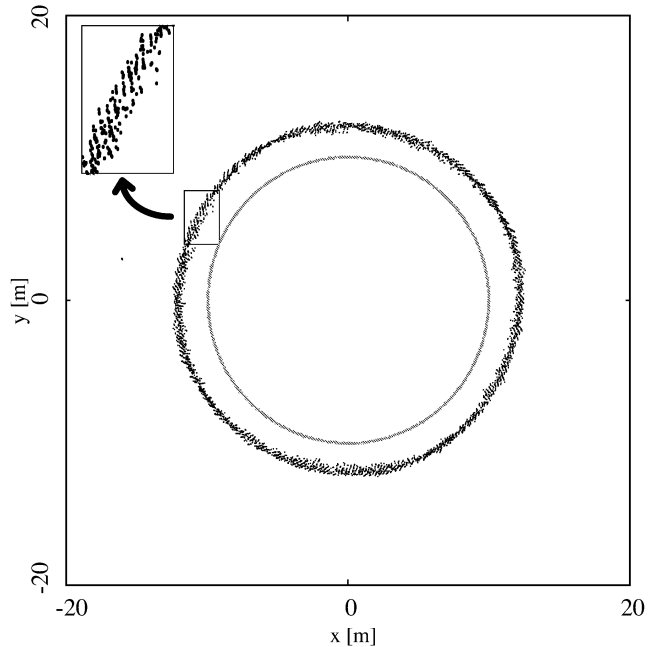


FIG. 1: Initial particle distribution (gray) and the same distribution after $23ns$ have elapsed. Parameters: $\zeta = 0.010$, $\gamma = 30$ and $v_{th} = 0.002$

is not possible to Fourier transform the charge perturbations in order to compute the growth rates for each value of m . Since the resolutions used were low the range of m values is restricted. Therefore, we will look at the saturation amplitudes and the radiated power instead which can be obtained easily. For larger energy spreads the bunching of the distribution becomes hardly visible, but it still can be observed in the z -component of the magnetic field (Fig. 2).

For a systematic analysis, the maximum electric field strength $|E|$ at any given time is determined and plotted vs. time in Fig. 3. The saturation is clearly visible, but the growth rate is two orders of magnitude higher than what would be expected from [1]. A possible explanation is that the ratio between the saturation amplitude and the electric self field

$$\left| \frac{\delta E_{sat}}{E_{self}} \right| = \frac{1}{m\zeta} \left(\frac{\Im(\omega)(m)}{\dot{\phi}} \right)^2 \quad (6)$$

is typically in the order of 10^{-3} for the given sample cases which is rather small. The initial perturbations due to discreteness, numerical noise etc. are usually in the same order of magnitude. Therefore, one cannot expect to see the regime covered by the linearized Vlasov equation. This is another reason for focusing entirely on the predicted saturation amplitudes and the emitted power. Subtracting the initial field amplitude from the saturation amplitude it is found that the saturation amplitude is proportional to γ (Fig. 3). A similar computation

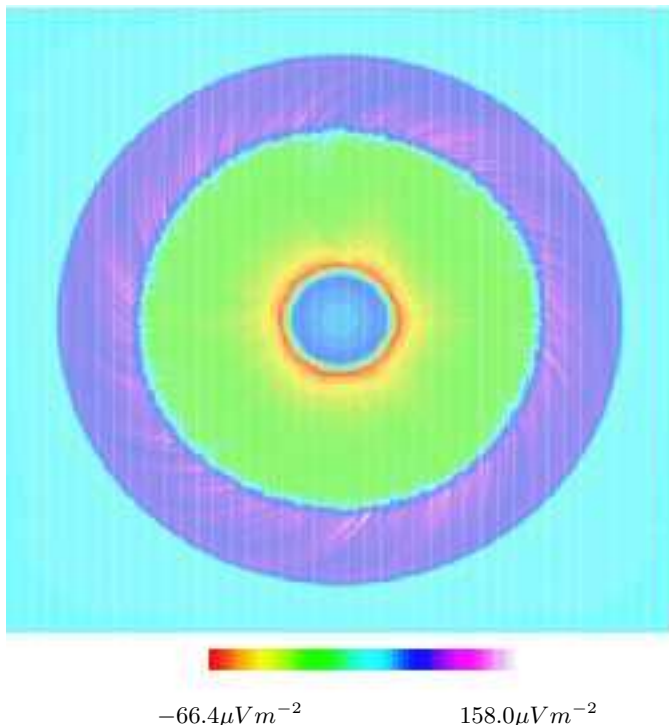


FIG. 2: z -component of the magnetic field (self-field plus perturbation without external magnetic field) after 23ns for $\zeta = 0.010$, $\gamma = 30$ and $v_{th} = 0.025$.

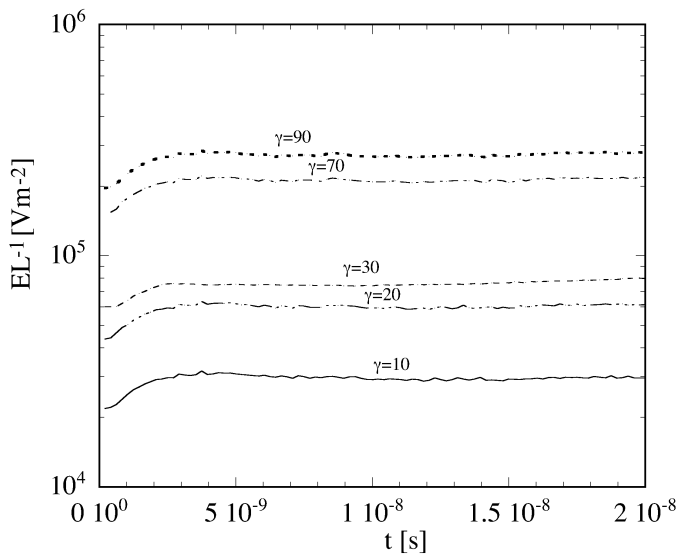


FIG. 3: Electric field strength E divided by L in $[\text{V m}^{-2}]$ vs. time t in $[\text{s}]$ for $\zeta = 0.02$, $v_{th} = 0.025$ and various values of γ .

shows that the saturation amplitude is also proportional to ζ , i.e. all relevant scalings which are expected from the analytical model are recovered.

In Fig. 4 the radiated power determined by measuring the kinetic energy loss of the electron cloud after approximately 2.36 ns is plotted as a function of ζ ; a quadratic

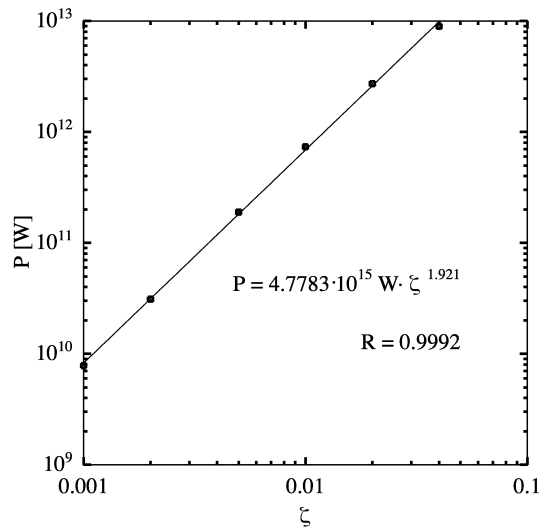


FIG. 4: Loss of kinetic energy in W vs. ζ for $\gamma = 30$ and $v_{th} = 0.025$. The solid line shows the best fit.

dependence can be established. Table I lists the same quantity determined under various conditions. From runs 145, 84 and 114 we see that the resolution of the grid does not affect the radiated power. This is consistent with the model [1] which predicts that most power is emitted by modes with low m . Also, decreasing the stepsize dt and increasing the number of macro particles has a negligible effect. Furthermore, the radiated power is proportional to ζ^2 and γ^2 . Thus, the dependence on ζ and γ agrees with [1]. In runs 77, 78 and 79 we increased the thermal energy spread, but kept all other parameters fixed. With increasing v_{th} the power decreases which is due to the decoherence predicted by Eq. 3.

Comparing runs 77 - 79 with runs 147 - 149, one concludes that the power scales as L^2 . This follows from the fact that $P \propto N^2$ and $N \propto L$. To determine the proportionality constant we look at runs 147 - 149 and evaluate the quoted expressions for the emitted power summing over all values of m . Fig. 5 compares the dependence of the emitted power on v_{th} computed by OOPIC and Eq. 2 starting to sum at $m = 1$. The upper limit is not critical since the power typically drops as $m^{-5/3}$, but half the number of lattice points pierced by a circle with radius r_0 is chosen, i.e. roughly 400. The values from Eq. 2 are the same order of magnitude as the values obtained from OOPIC. Note that Fig. 1 suggests $k_r v_{th} r_0 \sim 1$, whereas Eq. 2 was derived under the assumption $k_r v_{th} r_0 \ll 1$.

The particle in cell code OOPIC was used to simulate the evolution of density perturbations in a thin ring of charged particles which move in relativistic almost cir-

Run #	ζ	γ	v_{th}	P [W]	comments
70	0.005	30	0.002	4.66e11	
71	0.010	30	0.002	1.84e12	
74	0.010	10	0.002	2.03e11	
76	0.010	90	0.002	1.65e13	
82	0.002	30	0.025	2.96e10	
84	0.010	30	0.025	7.20e11	
87	0.020	10	0.025	3.00e11	
90	0.020	90	0.025	2.41e13	
77	0.010	30	0.002	1.28e12	
78	0.010	30	0.015	1.01e12	
79	0.010	30	0.033	6.01e11	
147	0.010	30	0.002	1.32e10	$L = r_0$
148	0.010	30	0.015	1.06e10	$L = r_0$
149	0.010	30	0.033	6.45e9	$L = r_0$
150	0.010	30	0.025	8.07e9	$L = r_0$
145	0.010	30	0.025	7.19e11	resolution = 256×256
84	0.010	30	0.025	7.20e11	resolution = 512×512
114	0.010	30	0.025	7.20e11	resolution = 1024×1024 , NMP= 50000, $dt = 2.5ps$

TABLE I: Loss of kinetic energy in $[Js^{-1}]$. The number of macro particles is denoted by NMP.

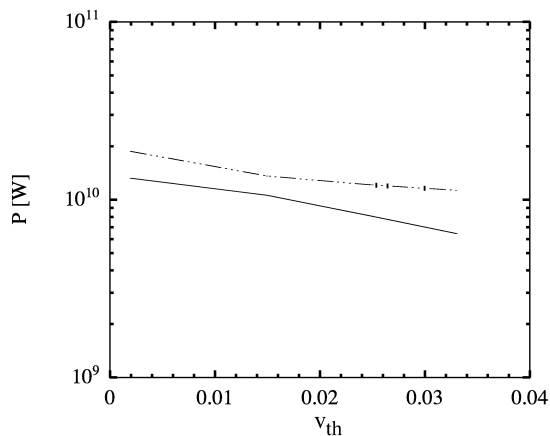


FIG. 5: Total power radiated as obtained from OOPIC (solid) and Eq. 5 with $m_1 = 1$ (dash-dotted) and $m_1 = \zeta^{3/2}\gamma^3 = 27$ (dotted)

cular motion in an external magnetic field. The results were compared with the model in [1]. Comparisons of the simulation with the model shows approximate agreement with the main predicted scaling relations. In particular the bunching effect could be observed very clearly and the emitted power is proportional to the square on the number density which implies coherent radiation.

I thank Richard V.E. Lovelace, Georg H. Hoffstaetter, Ira M. Wasserman and Joseph T. Rogers for valuable discussions and John Verboncoeur for his help with OOPIC. This work was supported by the US Department of Energy under cooperative agreement # DE-FC03-02NA00057.

* Electronic address: bss28@cornell.edu

- [1] Schmekel, B.S., Lovelace, R.V.E, Wasserman, I.M., preprint astro-ph/0409645
- [2] Goldreich, P., & Keeley, D.A. 1971, ApJ, 170, 463
- [3] A. Kabel, SLAC-PUB-9352 *Presented at IEEE Particle Accelerator Conference (PAC 2001), Chicago, Illinois, 18-22 Jun 2001*
- [4] J.P. Verboncoeur, A.B. Langdon and N.T. Gladd, Comp. Phys. Comm., 87, May 11, 1995, pp. 199-211
- [5] Jackson, J.D., Classical Electrodynamics, Wiley